Pis'ma v ZhETF, vol. 97, iss. 7, pp. 485 – 490 © 2013 April 10

Role of anion ordering in the coexistence of spin-density-wave and superconductivity in $(TMTSF)_2ClO_4$

Ya. A. Gerasimenko[+1)], *V. A. Prudkoglyad*[+], *A. V. Kornilov*[+], *S. V. Sanduleanu*[+*], *J. S. Qualls*[×], *V. M. Pudalov*[+*]

[+] *Lebedev Physical Institute of the RAS, 119991 Moscow, Russia*

[*] *Moscow Institute of Physics and Technology, 141700 Dolgoprudny, Russia*

[×] *Sonoma State University, Rohnert Park, CA 94928, USA*

Submitted 13 March 2013

Using various transport and magnetotransport probes we study the coexistence of spin-density wave and superconductor states in $(TMTSF)_2ClO_4$ at various degrees of ClO_4 anions ordering. In the two-phase complex state when both superconductivity and spin-density wave are observed in transport, we find prehistory effects, enhancement of the superconducting critical field, and strong spatial anisotropy of the superconducting state. These features are inconsistent with the conventional model of structural inhomogeneities produced by anion ordering transition. We reveal instead that superconductor and spin-density wave regions overlap on the temperature – dimerization gap V phase diagram, where V is varied by anion ordering. The effect of anion ordering on $(TMTSF)_2ClO_4$ properties is thus analogous to that of pressure on $(TMTSF)_2X$ ($X=PF_6$ or AsF_6), thereby unifying general picture of the coexistence of superconductivity and spin-density wave in these compounds.

DOI: 10.7868/S0370274X13070096

1. Introduction. For many unconventional superconductors including recently discovered Fe-based pnictides [1] the P–T phase diagram contains overlapping regions of the superconductor (SC) and antiferromagnetic insulator phase (here P is either external pressure, or internal "chemical" pressure, induced by chemical substitution or doping). The coexistence of the two phases causes unusual superconducting properties in the overlap region. Of a particular interest are quasi one-dimensional (Q1D) organic compounds of the $(TMTSF)_2X$-family [2]. The $(TMTSF)_2PF_6$ (hereafter PF6) was found to demonstrate rich physics near the spin-density wave (SDW) endpoint [2]. In the vicinity of the SDW transition the PF6 bulk homogeneous state is spontaneously split into SDW and metal/SC areas [3–5] with substantially enhanced superconducting critical field [6] and of strongly anisotropic shape [7]. The unusual SC behavior is believed to be due to curious properties of the SDW phase [8–10]. The latter is governed by nesting of the Fermi surface (FS), which easily occurs in Q1D compounds with two slightly corrugated FS sheets (cf. Fig. 1a). Application of pressure increases the dimensionality of electron dispersion (via increasing the $t'_b = t_b^2/t_a$ transfer integral), which spoils nest-

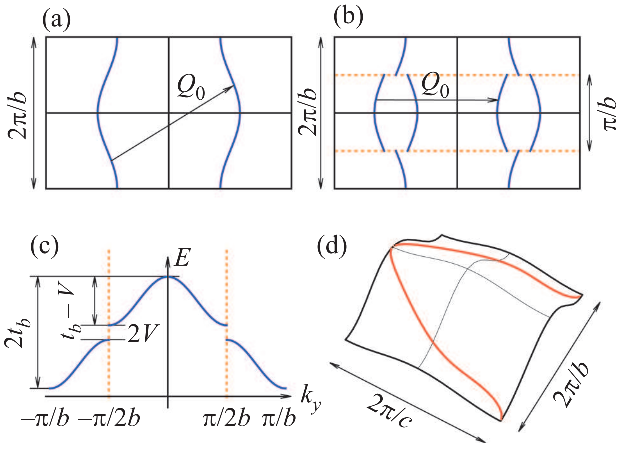

Fig. 1. (Color online) (a) – Fermi surface of PF6 or ClO4 in the absence of anion ordering. The wave vector Q_0 nests opposing sheets of the Fermi surface. (b) – Fermi surface of ClO4 in presence of anion ordering. Dashed line indicates the new Brillouin zone boundary due to doubled periodicity along b-axis. Now there are four sheets, which can be nested with Q_0 only when the splitting V is small. (c) – Sketch of the k_y bandwidth measured by AMRO with or without anion ordering. (d) – One sheet of the Fermi surface with the orbit (red line), that corresponds to the magnetic field aligned in the direction of zeroth order AMRO peak. The direction depends on k_y bandwidth

[1)] e-mail: gyaroslav@sci.lebedev.ru

ing and shifts formation of SDW to progressively lower temperatures.

In contrast, for apparently similar $(TMTSF)_2ClO_4$ (hereafter ClO4) compound, the SC/SDW coexistence is completely different. ClO_4 anions lack inversion symmetry, possess a dipole momentum, and experience ordering transition at $T_{AO} = 24\,K$. The transition doubles the lattice along b-axis and splits the Fermi surface in four open sheets (see Fig. 1b). The latter spoils nesting and suppresses SDW phase giving rise to the onset of superconductor state [2]. Due to finite time kinetics [11] of the anion ordering transition, the degree of anion ordering can be varied by adjusting the cooling rate in the vicinity of T_{AO}. This novel parameter enables to reveal a rich phase diagram, where SDW phase is favored for strong disorders, SC and SDW coexist at intermediate and SC sets in for weak disorders [12]. Earlier measurements with ClO4 did not reveal any features similar to those for PF6 and suggested that the SC/SDW coexistence is due to superconducting anion-ordered inclusions in the SDW insulating disordered background [12]. This was further supported by extensive X-ray measurements, where anion-ordered inclusions were indeed observed [11].

It was shown later, that the lower the SDW onset temperature, T_{SDW}, is, the stronger it is affected by magnetic field $\mathbf{H}\|c$ [13–15], consistent with the conventional mean-field description of SDW [16]. This, however, implies that some parameter, that spoils FS nesting, increases when T_{SDW} decreases. The latter occurs with lowering disorder, when only the FS splitting V is expected to change. Indeed, V plays the role similar to t_b' in PF6. For the strongest disorder the Fermi surface for ClO4 is similar to that for PF6 and can, thus, be nested (cf. Fig. 1a). Gradual ordering of anions splits the FS, and V represents the deviation from perfect nesting (cf. Fig. 1b). Imperfect nesting decreases T_{SDW}, until, at some disorder, the deviation reaches a critical value and SDW vanishes.

This simple picture is nicely supported by the mean-field calculations of the $T_{\mathrm{SDW}}(V)$ phase diagram [17, 18]. The similarity of SDW phase diagram to that of PF6 suggests, that the remarkable features of the SC and SDW coexistence should be observed also in ClO4, in contrast to a previously suggested picture of structurally inhomogeneous granular SC state [12]. Therefore, to resolve these conflicting views, it is necessary to study in detail the SC and SDW phase diagram as a function of V. Since V is expected to be spatially inhomogeneous due to structural disorder [11], it cannot be characterized by the residual resistivity or cooling rate at T_{AO} and should be measured directly.

In this paper we use several transport probes to characterize in real and momentum space the SDW and metal/SC coexistence for variable disorder. We use angular magnetoresistance oscillations for field rotated in the a–c-plane to probe the FS and trace changes in V. We indeed observe that V is reduced as T_{SDW} rises with increasing disorder, in accord with the theoretical phase diagram [17, 18]. We find that the SC phase is strongly spatially anisotropic: while transport along c-axis manifests survival of the SC state, the a-axis conduction turns out "insulating" with increasing disorder. For strong disorders we observed hysteresis in $R(T)$ behavior and enhancement of superconducting critical field, similar to that observed in PF6. These results clearly demonstrate that the metal/SC and SDW regions do overlap on the T–V phase diagram and their coexistence is driven by the changes of splitting V varied with the degree of anion ordering, rather than by structural inhomogeneities produced at anion-ordering transition.

2. Experimental. The single crystals of typical dimensions of $1 \times 0.15 \times 0.05\,\mathrm{mm}^3$ were synthesized using a conventional electrochemical technique. Eight $10\,\mu$m annealed Pt wires were glued with conducting graphite paint on two opposite crystal faces normal to c-axis. R_{xx} and R_{zz} resistances were measured along a and c-axes correspondingly using the conventional 4-wire AC technique. Samples were mounted on the ^{3}He one-axis rotator and cooled down to 40 K at the rate of 0.3 K/min to avoid cracks. Initially, to achieve the strongest disorder (d1) a heat pulse was applied to the continuously cooled ^{3}He bath at 1.3 K. This resulted in the bath heating well above T_{AO} and consequent rapid cooling at the rate of ≈100 K/min in the vicinity of T_{AO}. All the subsequent weaker disorders were obtained by annealing a sample at temperatures lower than T_{AO} [12]. The annealing procedure consisted in warming the sample to a certain temperature at the rate of 0.2 K/min and then cooling it back at the same rate. The highest annealing temperature corresponding to disorder d5 was 22 K. To achieve the anion-ordered state a sample was cooled from 40 to 20 K at the rate of 10 mK/min.

Samples were aligned in magnetic field by virtue of the upper critical field, H_{c2}, anisotropy; in the a–c crystal plane H_{c2} is the highest for $\mathbf{H}\|a$ and the lowest for $\mathbf{H}\|c$. Therefore, a-direction was determined using the resistance drop due to the onset of superconductivity on the rotation curve at a field value slightly lower than $\mathbf{H}_{c2}\|a$, and c-direction was set 90 degrees away.

3. Results and discussion. Figure 2 shows the intralayer R_{xx} temperature dependence for various disorders. For strong disorders the sample undergoes SDW transition ($T_{\mathrm{SDW}} = 6.6$ K for d1), followed by insulating temperature dependence of R_{xx} for lower temperatures. Upon decreasing disorder, SDW is suppressed, as seen from T_{SDW} decrease. For disorders d3, d4 transition becomes even more smeared, however the low-temperature behavior remains insulating and indicates the presence of SDW.

For strong disorders d1, d2, the $R_{xx}(T)$ behavior is insulating for $T < T_{\mathrm{SDW}}$, although there is a kink at ≈ 1.1 K which is followed by a slower growth of resistance. For weaker disorders d3, d4 the kink is followed by resistance drop. R_{xx} behavior below $T < 1.1$ K changes from yet insulating (d3) to already metallic (d4), however resistance stays finite down to the base temperature 0.4 K. Application of low magnetic field suppresses this feature and restores insulating behavior at low temperatures, as shown in the inset to Fig. 2. This indicates that

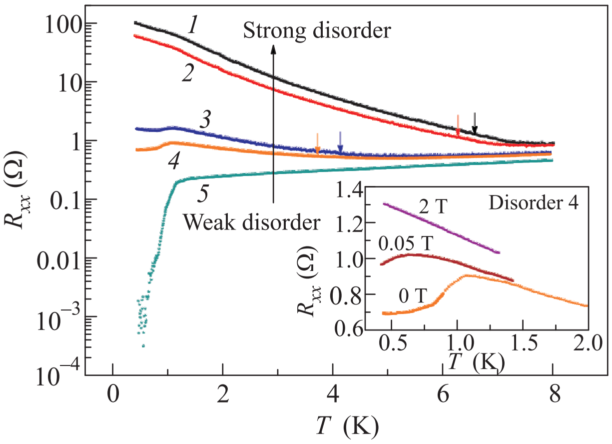

Fig. 2. (Color online) Temperature dependences of intralayer resistance R_{xx} for 5 different degrees of anion ordering. The colors are specific to each disorder on all figures hereafter. Arrows show the transition temperature T_{SDW} defined as a peak in the $d\ln R_{xx}/d(1/T)$ derivative. Inset shows the $R_{xx}(T)$ dependences in different magnetic fields $\mathbf{H}\|\mathbf{c}$ for disorder d4

the kink and the drop are associated with the presence of superconducting inclusions within the layers in the background SDW phase.

Finally, for the weakest disorder d5 insulating behavior is absent and superconducting transition is observed with intralayer resistance falling to zero. The overall behavior of R_{xx} is quite similar to the one observed previously by Schwenk et al. [12], where the authors came up with a model of a mixture of superconducting anion-ordered inclusions in the SDW background phase. The increase in the number and size of the inclusions with decreasing disorder (annealing the sample) leads to the percolating SC paths, the behavior similar to granular SC. The kink and the drop are then associated with the SC transition inside the inclusions, and the metallic temperature dependence that follows the drop indicates the developing percolating transition between the inclusions within the layers.

The interlayer, R_{zz}, resistance behavior is quite different from the intralayer one, as one can see from Fig. 3. The most prominent difference consists in full supercon-

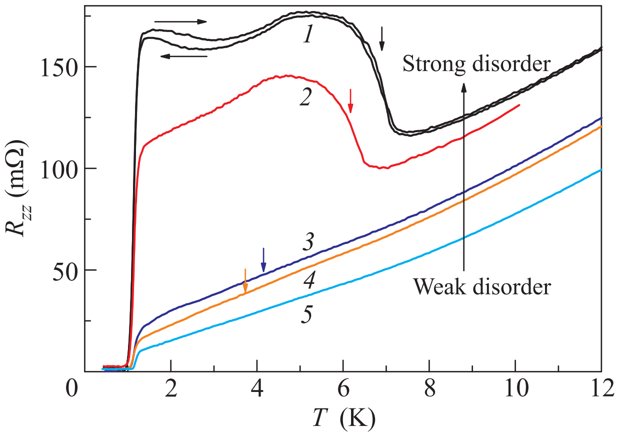

Fig. 3. (Color online) Temperature dependences of interlayer resistance R_{zz} for 5 different degrees of anion ordering. Arrows indicate SDW onset as seen in R_{xx}

ducting transition for all the disorders, even those where SDW is clearly observed in R_{xx}. In contrast to the two-step transition observed for $R_{xx}(T)$, e.g. d4, characteristic of a granular SC, the superconducting transition in $R_{zz}(T)$ is smooth. For strong disorders, the critical temperature $T_c \approx 1$ K is only slightly reduced compared to the ordered sample $T_c \approx 1.3$ K [2] and transition becomes wider. There are evidences [19–21] for nodal d-wave pairing in ClO4, therefore, T_c suppression is expected with increasing disorder. Note, that disorder changes R_{zz} almost by a factor of 3 (compare the d1 and d5 curves in Fig. 3 at $T = 10$ K).

The second difference is that the metallic behavior is preserved for R_{zz} even for those disorders, where R_{xx} is clearly insulating. The abrupt increase of R_{zz} resistance is observed for disorders d1, d2 at the same temperature, where the the SDW onset is observed in R_{xx}. However, the increase is absent for disorders d3, d4 (cf. Fig. 3). Such a behavior might be expected due to the cross-section squeezing of the current paths as soon as insulating background sets in.

The most remarkable result here is the hysteresis between the cooling and heating curves (cf. d1 curve on Fig. 3). Resistance is somewhat larger when the sample is heated from low temperatures, and the difference between the cooling and heating curves vanishes only at $T_{\rm SDW}$. The hysteresis in $R_{zz}(T)$ is a stationary effect and is not altered by either temperature sweep rate or the annealing time at $T < T_{\rm SDW}$. Anion ordering is not expected to change at temperatures much less than the gap. Indeed, annealing even at 10 K has virtually no effect on the low-temperature resistivity [12]. Due to strong disorder it is possible that some parts of the sample have lower local SDW transition temperature and thus become insulating at lower temperatures than the majority of a sample bulk. These structural inhomogeneities, however, cannot account for the hysteresis.

Alternatively, the hysteresis might occur when phase transition between the two neighboring phases, namely between metal and SDW is of the first order. In this case, inclusions of the minority phase are present atop the majority phase even below $T_{\rm SDW}$. The amount of minority phase vanishes with decreasing temperature and is not restored until the phase boundary is crossed again. The first order transition line was observed also by a number of probes in PF6 [3–5], where it leads to quite similar temperature hysteresis behavior in R_{zz} [6] in the SC/SDW coexistence region under pressure.

Deeper insight in the nature of metal and SDW coexistence can be obtained by probing the influence of disorder on the energy spectrum. Angular dependence of magnetoresistance is the major tool for obtaining information about the Fermi surface in quasi-one dimensional metals. Figure 4 demonstrates R_{zz} angular magnetoresistance oscillations (AMRO) for magnetic field rotated in the a–c-plane. As one can see from Fig. 4d, several pronounced peaks near $\mathbf{H}\|a$ are observed on the monotonic cosine background for a very weak anion disorder. This effect is well understood in terms of Boltzmann transport and results from vanishing average electron velocity $\langle v_z\rangle$ on certain type of orbits [22] (see Fig. 1d). The average $\langle v_z\rangle$ has the same zeros as the Bessel function $J_0(\frac{2t_bc}{\hbar v_f}\frac{B_x}{B_z})$, which corresponds to the orbits fitting the integer number of Brillouin zones along k_z (see cartoon on Fig. 1d) [22]. One can see, that the angular distance between the peaks is proportional to the k_y bandwidth $2t_b$. In the presence of anion ordering the bandwidth is $t_b - V$ (see Fig. 1c), thus by measuring the AMRO effect in the a–c-plane we can directly probe the changes in local value of V. The results are presented on Fig. 4 for a set of disorders, including those, where hysteresis in $R_{zz}(T)$ dependence is observed. The peaks are damped due to scattering time reduction at strong disorders, however zeroth-order peaks are still present. We observe that with increasing disorder the peaks are moving away from each other, directly indicating reduction of the band splitting V. Previous attempts [23] to observe the disorder dependence of V used the AMRO effect in the a–b-plane. The latter effect is due to small enhancement of conductivity for certain directions of magnetic field, nearly parallel to the velocities of the electrons in the inflexion points of FS [2]. This small enhancement is strongly damped by disorder thus making impossible observation of the a–b AMRO effect at strong disorder.

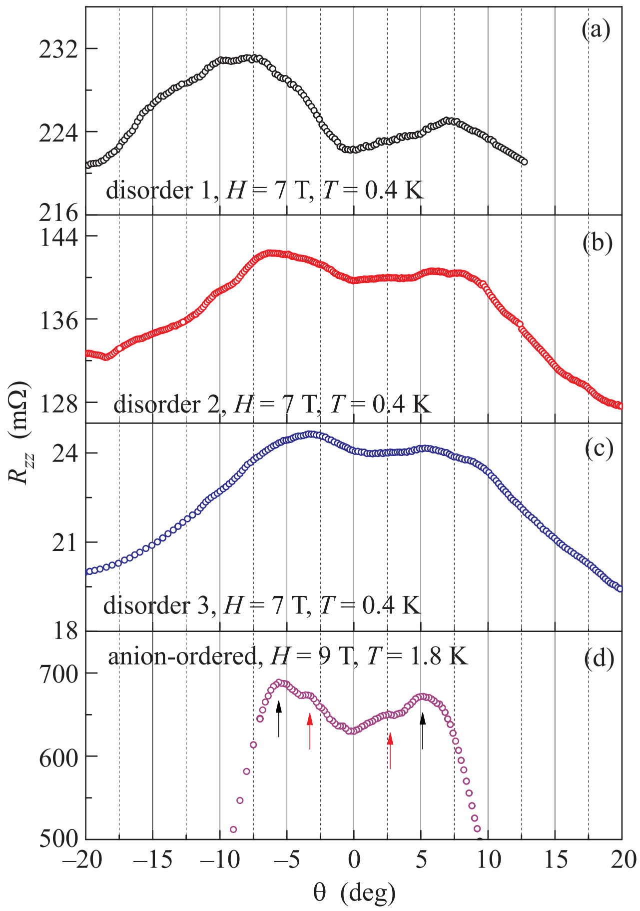

Fig. 4. (Color online) AMRO in the a–c plane for disorders *1–3* and for the anion-ordered state (from top to bottom). θ is the tilt angle of magnetic field with respect to the a-axis in the a–c-plane and is zero for $\mathbf{H}\|a$. Black and red arrows correspond to zeroth and first order oscillations. The disproportion of the resistance in symmetric peaks is due to presence of small magnetic field $\mathbf{H}\|b$, caused by slight misalignment of the sample

X-ray diffraction measurements [11] suggest that macroscopic anion-ordered grains are present even for rapidly cooled samples (i.e. at strong disorder). The SC ground state is certainly favorable inside the grains. Moreover, recent theoretical studies [24] also showed that d-wave SC can survive in ClO4 at strong disorder due to Josephson coupling between SC inclusions, provided the distance between them is of the order of the coherence length. Therefore, it is important to figure out the contribution of anion-ordered inclusions to the observed interlayer SC paths. The damped peaks in the a–c AMRO clearly indicate that the metallic/SC regions are disordered, and no additional peaks are observed at the angular position of $\theta = \pm 5.7°$, corresponding to the anion-ordered state (see Fig. 4). The latter implies that either their overall contribution to conductivity is small or their size is comparable to the mean free path. In any case, the interlayer SC paths are weakly influenced by the presence of anion-ordered inclusions.

Another probe for the two-phase SC/SDW state is its superconducting critical field. Figure 5 shows the

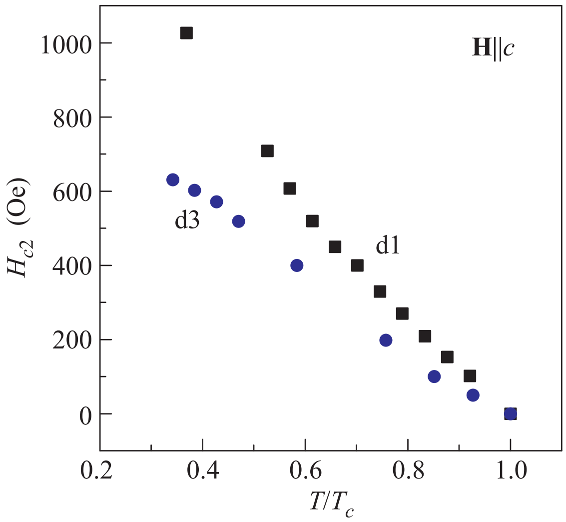

Fig. 5. Temperature dependence of critical field for disorders 1 and 3. The critical field was estimated as midpoint (50%) of the resistive transition

$\mathbf{H}_{c2}||c$ temperature dependences for two disorders, d1 and d3 in the coexistence region. For stronger disorders the $H_{c2}(T)$ curve shows a remarkable upturn, and the critical field becomes significantly enhanced compared to disorder d3. The positive curvature is absent for disorder d3, as well as for the ordered sample [2]. This indicates, that the H_{c2} upturn is a specific property of stronger disorders, where the presence of SDW stronger affects the SC phase.

In the Ginzburg–Landau theory the slope dH_{c2}/dT is related to the coherence lengths $\xi_i\xi_j$ in the plane normal to the magnetic field direction. For a granular superconductor the increase of slope is possible provided the size of grains is smaller than ξ, however neither $R_{zz}(T)$ nor AMRO measurements demonstrate the significant contribution of the anion-ordered grains to the interlayer metal/SC paths. For homogeneous superconductor, the disorder induced variation of V can change the effective mass and thus affect ξ. Indeed, the increase of the slope was observed for weak disorders [25], but it was much weaker compared to that for disorder d1. On the other hand, the coexistence of SC and SDW phases is expected to affect SC either in real (e.g. when the size varies due to self-consistent formation of spatially inhomogeneous state on the scale of $d \sim \xi$), or in momentum space (e.g. when the effective mass varies due to FS reconstruction by nesting). Thus, critical field enhancement provides the solid evidence of the SC/SDW coexistence.

The strong enhancement of $\mathbf{H}_{c2}||c^*$ was observed in $(TMTSF)_2PF_6$ [6] and was widely discussed theoretically [10, 26, 27]. Some theories [10, 26] predict such an enhancement due to the coupling of SDW and triplet SC order parameters. To our knowledge, no indication of triplet SC was ever observed in ClO4, and for anion-ordered ClO4 recent angular dependent specific heat measurements in magnetic field are in support of the nodal d-wave pairing [21]. Unless the character of pairing is changed by the onset of SDW state [26], the above scenarios [10, 26] are inapplicable to ClO4.

Another approach [27] suggests that SDW order parameter is non-uniform with domain walls separating neighboring regions with different order parameter. The domain walls can become superconducting, and critical field is enhanced due to their small cross-section. This approach also implies spatial anisotropy of the SC phase, since domain walls are normal to the a-axis. The latter is supported by recent transport anisotropy measurements in PF6 [7]. Resistivity anisotropy and critical field enhancement observed in this paper in ClO4 are also consistent with the domain walls scenario, though additional measurements are required to prove it.

In summary, using transport measurements and by varying anion disorder in $(TMTSF)_2ClO_4$ we probed the inner structure of its complex state where the SDW phase coexists with either SC phase (for $T < T_c$) or metallic phase (for $T > T_c$). The hysteresis in temperature behavior of interlayer resistance points to the first-order character of metal-SDW phase boundary. We find that the metallic/SC phase formed upon crossing this boundary is strongly spatially anisotropic. For strong disorders, it survives in a form of regions elongated at least in the interlayer (c) direction, whereas along the a-axis SDW insulating behavior is preserved. The critical field is enhanced in such a regions compared to the homogeneous SC state, which suggests that their cross-section decreases as SDW is stabilized by increasing disorder. At the same time, AMRO measurement in fields larger than H_{c2} show that in the metallic/SC regions ClO_4 anions are predominantly disordered and band splitting V is lower compared to the ordered state. Moreover, we directly observe that the latter is progressively reduced as disorder increases and SDW onset is shifted to higher temperatures. The above results demonstrate that SC/SDW coexistence in ClO4 is driven by the FS splitting V (similar to t_b' in PF6), rather than by structural inhomogeneities produced at the anion-ordering transition. This unifies the picture of SC/SDW coexistence in ClO4 and PF6 or AsF6. Thus, ClO4 represents a peculiar example, where competition between magnetic insulating and superconducting phases can be studied by continuous tuning of the degree of anion disorder.

Authors would like to thank P.D. Grigoriev and M.V. Kartsovnik for discussion of the preliminary results. The work was supported by RFBR, Programs of the Russian Academy of Sciences, by Russian Ministry for Education and Science (grant # 8375), and using research equipment of the Shared Facilities Center at LPI.

1. For a review see: M. V. Sadovskii, Uspekhi Fiz. Nauk **178**(12), 1243 (2008) [Phys.-Usp. **51**, 1201 (2008)].
2. For a review see: *The Physics of Organic Conductors and Superconductors* (ed. by A. Lebed), Springer-Verlag, 2008.
3. T. Vuletić, P. Auban-Senzier, C. Pasquier et al., Eur. Phys. J. B **25**, 319 (2002).
4. A. V. Kornilov, V. M. Pudalov, Y. Kitaoka et al., Phys. Rev. B **69**, 224404 (2004); Pis'ma v ZhETF **78**(1), 26 (2003) [JETP Lett. **78**(1), 21 (2003)].
5. I. J. Lee, S. E. Brown, W. Yu et al., Phys. Rev. Lett. **94**, 197001 (2005).
6. I. J. Lee, P. M. Chaikin, and M. J. Naughton, Phys. Rev. Lett. **88**, 207002 (2002).
7. N. Kang, B. Salameh, P. Auban-Senzier et al., Phys. Rev. B **81**, 100509 (2010).
8. D. Podolsky, E. Altman, T. Rostunov, and E. Demler, Phys. Rev. Lett. **93**, 246402 (2004).
9. L. P. Gor'kov and P. D. Grigoriev, Europhys. Lett. **71**, 425 (2005).
10. W. Zhang and C. A. R. Sá de Melo, Phys. Rev. Lett. **97**, 047001 (2006).
11. J.-P. Pouget, S. Kagoshima, T. Tamegai et al., J. Phys. Soc. Japan **59**, 2036 (1990).
12. H. Schwenk, K. Andres, and F. Wudl, Phys. Rev. B **27**, 5846 (1983); **29**, 500 (1984).
13. N. Matsunaga, A. Ishikawa, K. Nomura et al., Synth. Met. **103**, 2133 (1999).
14. N. Matsunaga, A. Briggs, A. Ishikawa et al., Phys. Rev. B **62**, 8611 (2000).
15. J. S. Qualls, C. H. Mielke, J. S. Brooks et al., Phys. Rev. B **62**, 12680 (2000).
16. G. Montambaux, Phys. Rev. B **38**, 4788 (1988).
17. D. Zanchi and A. Bjelis, Europhys. Lett. **56**, 596 (2001).
18. K. Sengupta and N. Dupuis, Phys. Rev. B **65**, 035108 (2001).
19. N. Joo, P. Auban-Senzier, C. R. Pasquier et al., Eur. Phys. J. B **40**, 43 (2004).
20. N. Joo, P. Auban-Senzier, C.R. Pasquier et al., Europhys. Lett. **72**, 645 (2005).
21. S. Yonezawa, Y. Maeno, K. Bechgaard, and D. Jérome, Phys. Rev. B **85**, 140502(R) (2012).
22. G. M. Danner, W. Kang, and P. M. Chaikin, Phys. Rev. Lett. **72**, 3714 (1994).
23. H. Yoshino, S. Shodai, and K. Murata, Synth. Met. **133–134**, 55 (2003).
24. S. Haddad, S. Charfi-Kaddour, and J.-P. Pouget, J. Phys. Cond. Mat. **23**, 464205 (2011).
25. C. P. Heidmann, H. Schwenk, K. Andres, and F. Wudl, Z. Phys. B **58**, 7 (1984).
26. P. D. Grigoriev, Phys. Rev. B **77**, 224508 (2008).
27. P. D. Grigoriev, Physica B **404**, 513 (2009).